Earth and Planetary Science Letters 579 (2022) 117346

Contents lists available at ScienceDirect

Earth and Planetary Science Letters

www.elsevier.com/locate/epsl

Gaining from loss: Detrital zircon source-normalized α-dose discriminates first- versus multi-cycle grain histories

Maximilian Dröllner *, Milo Barham, Christopher L. Kirkland

Timescales of Mineral Systems Group, School of Earth and Planetary Sciences, Curtin University, GPO Box U1987, Perth, WA 6845, Australia

ARTICLE INFO

Article history:
Received 12 May 2021
Received in revised form 23 November 2021
Accepted 13 December 2021
Available online 27 December 2021
Editor: A. Webb

Keywords:
U–Pb geochronology
sediment routing
sedimentary recycling
metamict
zircon chemistry
alpha dose

ABSTRACT

Detrital zircon U–Pb ages are widely employed as an archive of geological processes through time. Changes in detrital zircon age patterns within sediments reflect changes in source areas that are often related to tectonic and/or climatic processes. However, discrimination of first-cycle and multi-cycle detrital zircon with primary crystalline and secondary sedimentary sources, respectively, can be challenging using only crystallisation age constraints. Here, we present U–Pb geochronology of detrital zircon from modern fluvial and littoral environments on the Scott Coastal Plain in Western Australia to investigate the use of α-dose to identify sedimentary recycling. The majority of 1032 concordant U–Pb ages are interpreted to be ultimately sourced from the local basement. However, U–Pb ages do not reflect the areal extent of source rocks and indicate significant reworking of coastal plain sediments. A novel metric – source-normalized α-dose – demonstrates predominant detrital zircon routing via recycling through intermediate storage. This metric is defined as the ratio of the average α-dose (a measure of metamictization) of detrital zircon belonging to a characteristic age group and the average α-dose of zircon grains within the corresponding source crystalline basement. Average values of source-normalized α-dose of detrital zircon populations <1 are interpreted to reflect selective removal of more labile (metamict) grains via attrition and diagenesis, indicating greater grain transport and recycling, whereas values of *c.* 1 signify shorter transport and a first-cycle origin. Application of this approach to ancient clastic systems is supported by consistency of results with independent indicators of progressive sedimentary recycling and/or transport. Source-normalized α-dose is an internal measure using zircon grain chemistry (U and Th), and avoids bias associated with multi-mineral measures of sediment recycling that may be related to source fertility. Additionally, source-normalized α-dose uses measures typically captured during routine U–Pb geochronology. Source-normalized α-dose of detrital zircon provides an additional method to address sedimentary source-to-sink transport and recycling, and ultimately allows more robust interpretation of U–Pb zircon data.

1. Introduction

Provenance analysis using detrital zircon (DZ) U–Pb geochronology is widely employed in reconstructions of ancient sediment routing systems (e.g., Dickinson and Gehrels, 2008), and in the understanding of tectonic and climatic processes (e.g., Huber et al., 2018). However, interpretation of DZ can be limited by the supply of multi-cycle DZ grains due to their physical and chemical stability, effectively masking propagation of geological signals from source-to-sink (e.g., Barham et al., 2021; Romans et al., 2016). Changes in the DZ signature in basins do not necessarily reflect coeval changes in their source areas, and primary signals may instead be overprinted or buffered by intermediate sediment reservoirs and processes intrinsic to the sedimentary system (autogenic). Thus, a major challenge in DZ studies is the discrimination of first- and multi-cycle detritus (e.g., Meinhold et al., 2011), i.e., sediment cargo derived directly from crystalline basement and intermediate sedimentary reservoirs, respectively.

Geological setting represents a first-order control on DZ composition (Cawood et al., 2012), and governs the propagation of environmental signals (e.g., variations in sediment production due to uplift) through a sedimentary system (Romans et al., 2016). Although some sedimentary systems display rapid signal responses (e.g., Covault et al., 2010), even mountainous sediment routing systems may involve intermediate sediment storage with residence times exceeding 100 kyr (e.g., Blöthe and Korup, 2013). While such relatively short periods may be less significant within the deep-time sedimentary record (>10^7 yr), other systems, such as

* Corresponding author.
E-mail address: maximilian.droellner@postgrad.curtin.edu.au (M. Dröllner).

https://doi.org/10.1016/j.epsl.2021.117346

coastal plains or sedimentary basins in general, enable significantly longer-term storage and recycling, thus decoupling detrital mineral age signatures from geological processes driving sediment production within crystalline source regions (Phillips and Slattery, 2006). Ultimately, this process will impede primary basement signal propagation by introducing significant lag times, effectively suppressing the detrital record of processes external to the sedimentary system (allogenic) (e.g., Fülöp et al., 2020). Capturing sediment storage and reworking is critical given these processes significantly influence (bias) geological interpretations (Chew et al., 2020).

Although the significance and implications of recycling, i.e., burial and re-exposure to erosion, within sedimentary systems have been recognized for several decades (Blatt, 1967), identification and quantification of sedimentary recycling remains challenging. Capturing the multicyclic nature of DZ can be achieved by integrated analysis of more labile mineral phases along with zircon (e.g., feldspar; Tyrrell et al., 2009) or in combination with mineral phases growing during diagenetic or low-grade metamorphic conditions (e.g., monazite; Zotto et al., 2020). However, integrated attempts using other mineral phases associated with DZ may suffer from source compositional bias, only indirectly inform about sourcing of DZ via sedimentary recycling, and cannot differentiate first- and multi-cycle zircon grains within the DZ population. While the integration of (U–Th)/He thermochronology and U–Pb geochronology of DZ can distinguish contributions of individual zircon grains derived by sedimentary recycling (e.g., Rahl et al., 2003), the "double dating" approach remains time- and labour-intensive, restricting its use in high-*n* studies. Resentini et al. (2020) have recently integrated Raman spectroscopy and laser ablation-inductively coupled plasma-mass spectrometry (LA-ICP-MS) U–Pb geochronology to distinguish sub-populations of DZ based on grain thermal histories and degree of metamictization. Metamictization, i.e., self-irradiation damage of the crystal lattice by radioactive decay, progressively lowers crystallinity, forming metamict (amorphous) zones in zircon (Nasdala et al., 2001). Ultimately, metamictization reduces chemical and structural robustness of zircon (Balan et al., 2001; Chakoumakos et al., 1987). Findings by Markwitz and Kirkland (2018) and Resentini et al. (2020) suggest selective removal of progressively more metamict zircon grains during sedimentary transport and recycling, which in turn is reflected by the decline of zircon grains displaying high α-dose (i.e., high number of α-decay events). Thermal annealing, as part of the grain history, may prevent the loss of crystallinity (Nasdala et al., 2001). Therefore, healing of radiation damage, e.g., during episodes of exposure to higher temperatures, may preserve high α-dose zircon grains. An absolute measure of crystallinity (and hence, metamictization) requires additional analysis (e.g., Raman). However, U and Th concentrations of DZ are commonly measured during conventional U–Pb geochronology of zircon grains, and together with age information can be used to calculate an apparent α-dose as a first-order proxy of metamictization (Murakami et al., 1991). Using an intrinsic internal measure to address sedimentary recycling of DZ, such as α-dose, makes subsequent interpretation independent of assumptions about relationships to other mineral phases and their shared origins. In addition, α-dose can be calculated for previously analysed materials and employed in future works with no modification to existing approaches.

This study employs DZ U–Pb geochronology to test the use of α-dose as a proxy of sediment transport and recycling in DZ. To decipher variations of DZ α-dose in the sedimentary system, we (i) devised a high-density sampling strategy of littoral and fluvial environments in a modern, discrete coastal plain with well-characterised crystalline basement hinterland in southwest Western Australia, and (ii) normalized α-dose values of DZ to the average α-dose of the corresponding source rock. We interpret the dominant controls on DZ composition and implications for provenance analysis through the geological record.

2. Geological setting

The Scott Coastal Plain (SCP) in SW Australia (Fig. 1) covers an area of ca. 1000 km^2 characterized by Cenozoic, dominantly siliciclastic sands containing heavy mineral sand placer deposits of economic relevance (Baxter, 1977). The coastal plain comprises several unconsolidated to well-consolidated transgressive dune and shoreline systems of variable thickness unconformably overlying Palaeozoic to Mesozoic rocks of the Perth Basin (Baddock, 1995). Drainage systems with catchments of variable size and sediment supply (Q_s) flow across the SCP and ultimately discharge into the Southern Ocean (Fig. 1B). The largest outlet is the Hardy Inlet estuary located at the western end of the study area. The Hardy Inlet is the confluence of the largest river system, the Blackwood River, and the Scott River. The eastern SCP is drained by two isolated, relatively minor river systems, the Donnelly River, and the Warren River. The coast in SW Australia is interpreted to get limited supply of terrigenous material by fluvial discharge (Short, 2010). The microtidal coast is wave-dominated by the high energy south-westerly swell (Fig. 1C) of the Southern Ocean that also transports sand onshore forming coastal dune systems (Short, 2010).

The crystalline basement bounding the study area consists of the Neoproterozoic-Palaeozoic Pinjarra Orogen (PJO), the Proterozoic Albany–Fraser Orogen (AFO), and the Archean Yilgarn Craton (YC) (Fig. 1C). The YC is the dominant lithology by area in SW Australia, and is subdivided into several terranes, with the South West Terrane most proximal to the sample sites. Zircon grains derived from the South West Terrane mainly formed during the Meso-Neoarchean at *c.* 2700–2600 Ma (Mole et al., 2019). The South West Terrane and the AFO create the eastern boundary of the SCP. The AFO represents the Proterozoic modification of the YC margin and is characterized by zircon age modes of 1710–1650 Ma, 1345–1260 Ma, and 1215–1140 Ma (Kirkland et al., 2011). The PJO crops out sporadically in the form of a few inliers along the western margin of Australia, such as the Leeuwin Complex, which is a promontory forming the western border of the SCP (Fig. 1A). The Leeuwin Complex records ages at *c.* 1100–1000 Ma, *c.* 750 Ma, and *c.* 520 Ma (Collins, 2003).

3. Material and methods

Fifteen samples were collected from different environments of the SCP in order to establish the spatial variation of DZ age populations within the system (Fig. 1C). Fourteen samples represent modern sediments, with one taken from a beachrock (quartzose calcarenite) at Flinders Bay (sample FLD005) assumed to be part of the Tamala Limestone (late Pleistocene; Baddock, 1995). Sampling was focused on drainage systems (Hardy Inlet estuary and Blackwood, Scott, Donnelly, Warren rivers) to capture sediment discharge, and littoral sediments to resolve DZ variations along the coast, with a single coastal dune sample (FLD004). All fluvial samples were derived from sand bars. All modern littoral samples were collected from the swash zone. Sample locations and brief descriptions are given in Supplementary Table S1 in Supplementary Material S2.

Sample handling was conducted with consideration of minimizing methodological bias and sample treatment. The grains of the consolidated beach rock sample (FLD005) were liberated using high voltage electrical fragmentation (selFrag Lab, Switzerland). All samples were processed using a riffle splitter to obtain representative material. Samples were sieved using a 500 μm mesh. About one kilogram of the $<$500 μm fraction underwent heavy mineral

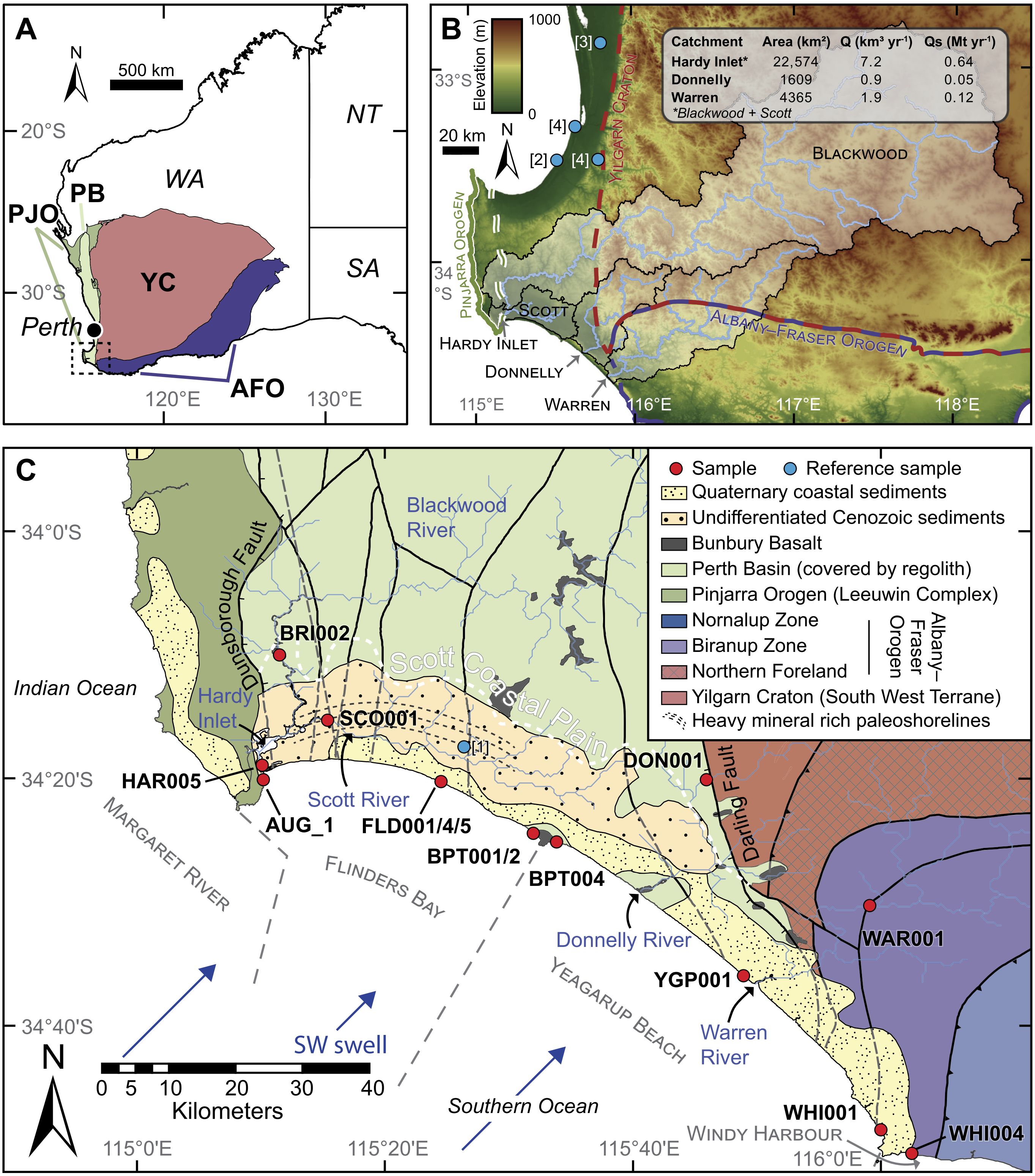

Fig. 1. (A) Location of study area (dashed rectangle) and onshore areal extent of relevant lithologies discussed in this study; PB – Perth Basin, PJO – Pinjarra Orogen; AFO – Albany-Fraser Orogen; YC – Yilgarn Craton; WA – Western Australia, NT – Northern Territory, SA – South Australia. (B) Digital elevation model of study area with catchments of drainage systems studied in this work; dashed lines indicate crystalline basement. Area, Water discharge (Q), and total suspended sediment load (Qs) derived from the global terrestrial sink catchment (GTSC) database (Nyberg et al., 2018); Qs calculated using the BQART formula of Syvitski and Milliman (2007). (C) Geological map of study area. Physiographic extent of Scott Coastal Plain (after Baddock, 1995) is indicated by dashed white line. Sample locations are indicated with a red dot (names corresponding to sample IDs are provided in Fig. 2). Dashed grey lines (offshore) indicate secondary coastal compartments following the nomenclature by Eliot et al. (2011). Blue dots and square brackets in (B) and (C) indicate positions of references used in Fig. 3. (For interpretation of the colours in the figure(s), the reader is referred to the web version of this article.)

separation using the Jasper Canyon Research (JCR) water-shaking table (Dumitru, 2016), heavy liquid separation at 2.85 g/cm^3, and a single-step separation using the Frantz isodynamic magnetic separator to enrich zircon content. A split (coning and quartering) of this zircon-rich separate was bulk-mounted, i.e., grains were embedded in epoxy resin in a 25 mm diameter mount and polished to maximum exposure. Zircon grains were identified utilizing automated mineral identification based on energy-dispersive X-ray spectrometry using a TESCAN Integrated Mineral Analyzer (TIMA). To avoid mixtures of age components, cathodoluminescence imaging using a TESCAN Clara FE-SEM was performed before analysis. Cores (where texturally relevant) of DZ have been selected for spot analysis to allow correlation of DZ to their ultimate source rock. Zircon grains were analysed by laser ablation-inductively coupled plasma-mass spectrometry (LA-ICP-MS) at Curtin University's John de Laeter Centre (Perth, Australia). Full documentation of analytical procedures is provided in Supplementary Material S1. The α-dose was calculated for each concordant analysis following Murakami et al. (1991), using the Eq. (1) modified after Holland and Gottfried (1955).

$$D = 8\frac{X_U \times N_A \times 0.9928}{M_{238} \times 10^3} \times [\exp(\lambda_{238}t) - 1] + 7\frac{X_U \times N_A \times 0.0073}{M_{235} \times 10^3}[\exp(\lambda_{235}t) - 1] + 6\frac{X_{Th} \times N_A}{M_{232} \times 10^3}[\exp(\lambda_{232}t) - 1] \quad (1)$$

D (α-dose) corresponds to the α-decay events/mg. X_U and X_{Th} are U and Th concentrations (in ppm); t = age (in Ma); N_A is the Avogadro constant; M_{238}, M_{235}, and M_{232} are the isotopic masses of ^{238}U, ^{235}U, and ^{232}Th, respectively; λ_{238}, λ_{235}, and λ_{232} are the decay constants (in yr^{-1}) for ^{238}U, ^{235}U, and ^{232}Th, respectively. The calculation assumes natural abundances of ^{238}U (*c.* 0.9928) and ^{235}U (*c.* 0.0073) isotopes based on a ^{238}U/^{235}U ratio of 137.88 (Steiger and Jäger, 1977). We calculated a new metric – source-normalized α-dose – for individual zircon grains based on the interpretation of their ultimate source rock (see section 5.1) by normalization to the median of the α-dose of zircon grains from their interpreted source rock, i.e., a value of 1 indicates similar α-dose values of DZ and grains in the interpreted crystalline source. Source rock data were compiled from primary crystalline basement rocks obtained from the geochronological database of the Geological Survey of Western Australia (http://dmp.wa.gov.au/geochron).

4. Results

In total, 1032 concordant DZ U–Pb ages were obtained (Fig. 2). The ages range from Paleoarchean to early Phanerozoic. The predominant age modes are at *c.* 730–500 Ma, *c.* 1100–880 Ma, *c.* 1240–1120 Ma, *c.* 1700–1600 Ma, and *c.* 2710–2580 Ma. These age modes represent *c.* 88% of the total age spectra measured. The 730–500 Ma age mode accounts for *c.* 52% of all ages. The youngest and oldest concordant zircon grains are 408 Ma (sample SCO001) and 3533 Ma (sample BPT001), respectively. Full documentation of DZ U–Pb ages are given in Supplementary Table S2 in Supplementary Material S2.

4.1. Fluvial samples

The DZ age distributions in the fluvial samples in the western and eastern SCP differ significantly (Fig. 2). The western drainage systems (Blackwood and Scott rivers) both show a prevalence of early Mesoproterozoic-Phanerozoic ages (1100–500 Ma; *c.* 72%) and minor occurrences of 1240–1120 Ma and 2710–2580 Ma age

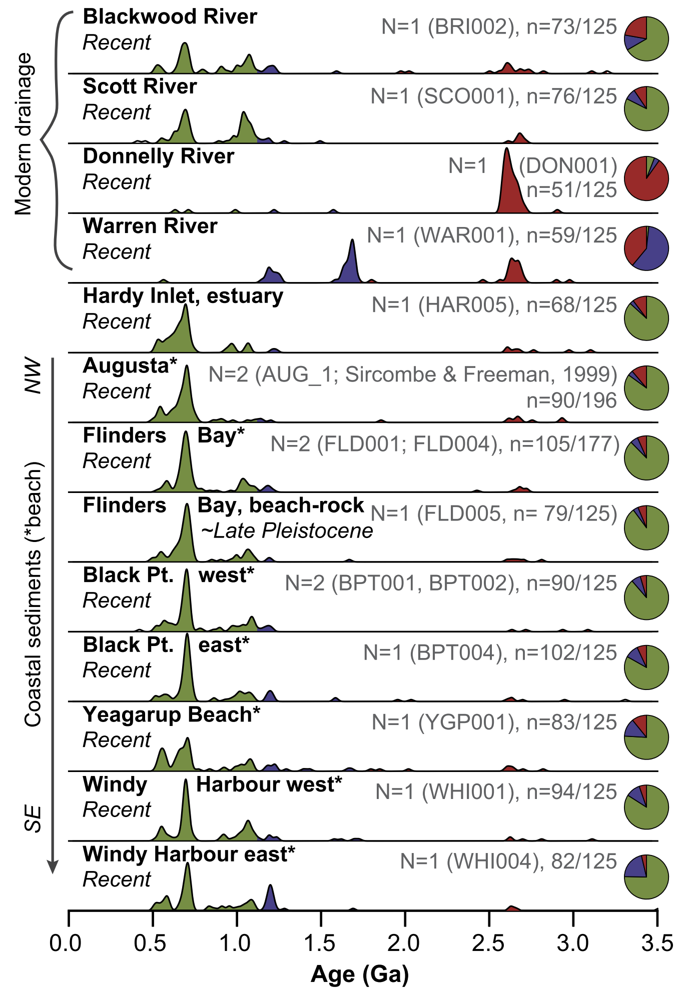

Fig. 2. Normalized kernel density estimates (bandwidth 15 Myr) of DZ U–Pb ages of the study area; Augusta sample of Sircombe and Freeman (1999) is from a similar location as sample AUG_1; N – number of samples; n – number of analyses (concordant/total). Interpretation of source is colour-coded: green – Pinjarra Orogen; blue – Albany-Fraser Orogen; red – Yilgarn Craton.

modes. The Hardy Inlet estuary (confluence of Blackwood and Scott rivers) presents a similar DZ spectra, but with a more pronounced dominance of DZ ages between 1100 and 500 Ma (*c.* 87%). The eastern rivers show distinct DZ populations. The Donnelly River is dominated by DZ ages between 2710 and 2580 Ma (*c.* 82%). The Warren River has a greater variety of ages but higher abundances of DZ ages at 1240–1120 Ma (*c.* 14%), 1700–1600 Ma (*c.* 37%), and 2710–2580 Ma (*c.* 31%). Both eastern rivers (Donnelly and Warren) document no, or only very little, 730–500 Ma and 1100–880 Ma DZ age modes.

4.2. Littoral samples

The modern littoral samples show qualitatively similar polymodal age distributions with the 730–500 Ma and 1100–880 Ma age modes dominating throughout (*c.* 70–82%). Age modes 1240–1120 Ma, 1700–1600 Ma, and 2710–2580 Ma are minor components. Beachrock sample FLD005 DZ shows a high similarity to the modern littoral DZ composition. From west to east the early Mesoproterozoic-Phanerozoic grains (age modes 730–500 Ma, 1100–880 Ma) decrease in abundance whereas older age modes 1240–1120 Ma and 1700–1600 Ma increase.

5. Discussion

Understanding of DZ sources (section 5.1) and local controls on the spatial variation of age modes (5.2 and 5.3) are required to understand and assess the utility of metrics for gauging the degree of recycling within DZ systems. Therefore, potential DZ sources (section 5.1) and the sedimentological controls on the DZ age distributions (5.2 and 5.3) are established at the outset. These sections allow the contextualization of the relationships relevant for subsequent discussion of the significance of the source-normalized α-dose metric (5.4) and its potential use in ancient sedimentary systems (5.5).

5.1. Potential sources of detrital zircon

The well-established geology of the study area allows for confident correlation of major DZ ages with regional crystalline basement source rocks that have been defined using a multi-decade sensitive high-resolution ion microprobe (SHRIMP) zircon geochronology program. Age modes at 730–500 Ma and 1100–880 Ma are assigned to the PJO (Collins, 2003). Age modes at 1240–1120 Ma and 1700–1600 Ma are related to derivation from the AFO (Kirkland et al., 2011). The YC is interpreted as the source of 2710–2580 Ma grains (Mole et al., 2019).

Potential sources of recycled DZ are the Perth Basin and the often poorly consolidated Cenozoic sediments of the coastal plain. Perth Basin DZ populations show significantly higher proportions of Mesoproterozoic and Archean ages (Fig. 3A) compared to most samples of this study (Fig. 2). Therefore, based on quantitative differences and limited exposure of the Perth Basin in proximity of the study area, Perth Basin sediments are unlikely to represent immediate sources of DZ. The similarity of DZ compositions of coastal sediments to those of Cenozoic paleo-shoreline sediments on the SCP (reference [1] in Fig. 3A) suggest a closer relationship, perhaps by sedimentary recycling, consistent with Kolmogorov–Smirnov (K–S) statistics (Fig. 3B).

5.2. Do rivers reflect their catchment geology?

The eastern and western drainage systems of the SCP show significant differences in their DZ populations and areal distribution of source rocks within their catchments (Fig. 4A). The Donnelly and Warren River DZ populations correlate to the relative spatial distribution of source rocks in their respective catchments. This supports direct sourcing of the DZ cargo in the eastern rivers, i.e., high degree of first-cycle sands, or absence of recycled or exotic material. In contrast, the relative proportions of DZ age modes in the Blackwood and Scott river samples do not correspond to the spatial extent of relevant source rocks within their catchments. For instance, the PJO occurs in less than 1% of the area of the catchment but is the ultimate source of the majority of the DZ ages (*c.* 75%; Fig. 4A). The opposite is observed for the YC. Although being the most extensive crustal component (*c.* 90%) in the catchment, only *c.* 9% of DZ ages in the Scott-Blackwood samples can be linked to the YC.

The mismatch between the representation of crustal units within DZ age populations and areal extents within the hinterland catchment of the largest sediment drainage system (based on sediment supply Q_s and catchment area) can be attributed to a combination of (i) zircon fertility (e.g., Moecher and Samson, 2006), (ii) erosion rates (e.g., Spencer et al., 2018), and (iii) sedimentary recycling (e.g., Meinhold et al., 2011). Although the zircon fertility, constrained by the Zr content of source rocks, is significantly higher in the PJO (*c.* 4:2:1 ratio to AFO and YC), zircon fertility cannot entirely account for the observed dominance of PJO-derived DZ given a *c.* 5:1:1 ratio to AFO- and YC-derived

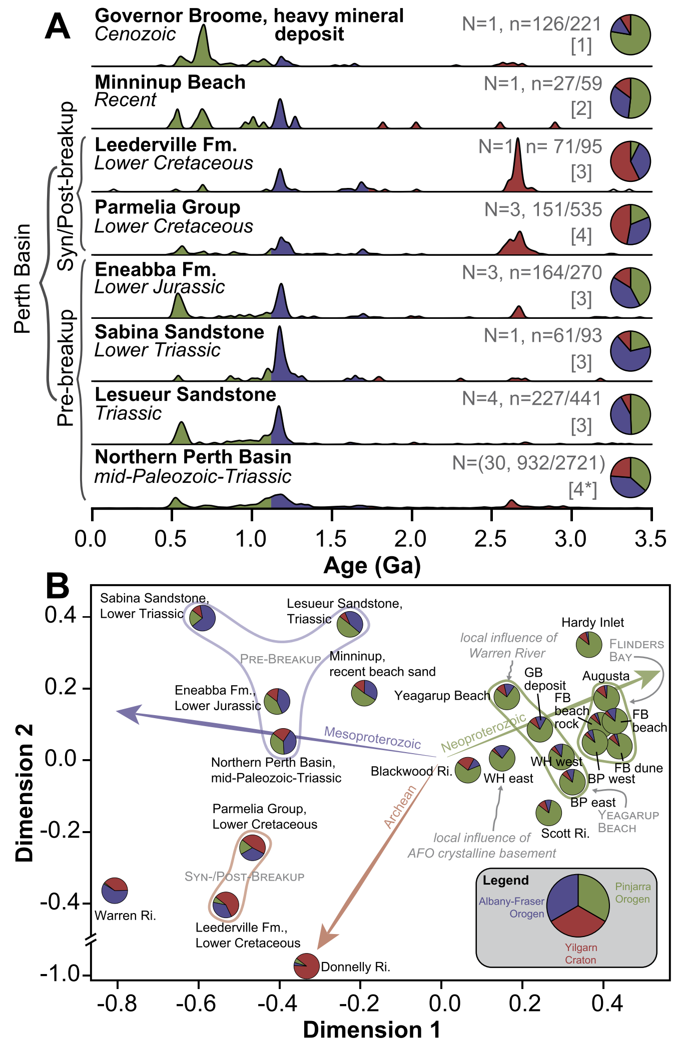

Fig. 3. (A) Normalized kernel density estimates (bandwidth 15 Myr) of DZ age spectra of relevant reference samples; N – number of samples; n – number of analyses (concordant/total). Interpretation of source is colour-coded: green – Pinjarra Orogen; blue – Albany-Fraser Orogen; red – Yilgarn Craton; [1] – sample GB001 (bulk-mounted) from Dröllner et al. (2021), [2] – Sircombe and Freeman (1999), [3] – Lewis (2017), [4(*)] – Olierook et al. (2019) *and references therein. (B) Multidimensional scaling using K–S statistics of DZ age spectra of samples of this study and Perth Basin sediments of different age. GB – Governor Broome; FB – Flinders Bay; BP – Black Point, WH – Windy Harbour, AFO – Albany-Fraser Orogen; Ri. – River, Fm. – Formation.

DZ in the Blackwood and Scott rivers samples (Fig. 4). Equally, significantly higher erosion rates for the onshore PJO within the drainage systems are unlikely to explain the great differences. Enhanced erosion rates are more likely to occur in the incised upper reaches, but lithologies of the upper reaches (YC) are the least represented sources. In addition, the passive margin setting displays negligible differences in topography and erosivity of the different source rocks (based on lithology factor after Syvitski and Milliman, 2007). However, the supply of multi-cycle detritus of sediments is expected to exceed primary supply from denudation of crystalline basement (first-cycle) in drainage systems such as the Blackwood River, which meanders through a variably consolidated sediment veneer (e.g., Fülöp et al., 2020). In fact, the Blackwood and Scott river samples DZ composition shows striking similarity with Cenozoic SCP sediments (Fig. 3A) suggesting sedimentary recycling is a key control of the DZ composition of the western drainage systems. Active recycling processes are supported by the presence of AFO-derived DZ despite a lack of corresponding sources in the catchment. Comparison of relative DZ abundances also implies

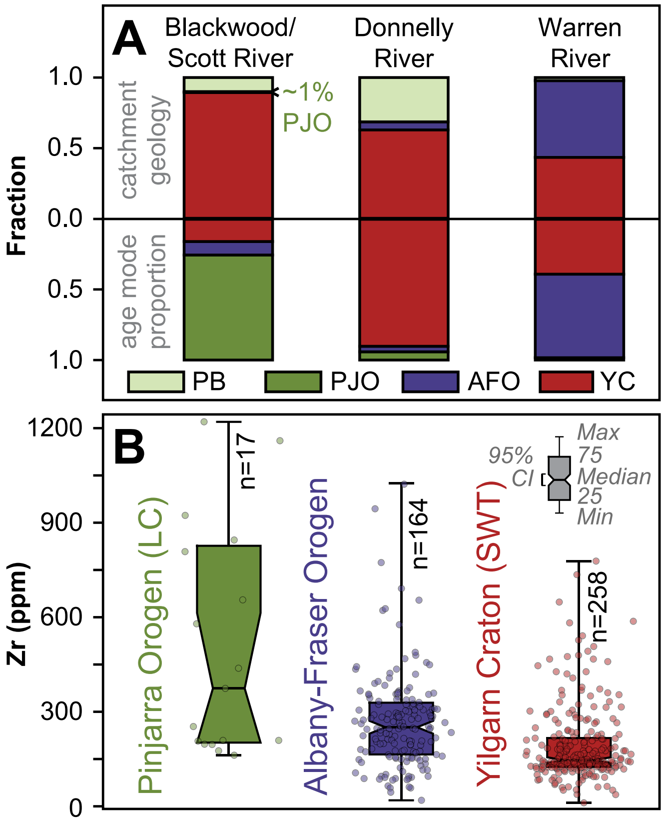

Fig. 4. (A) Comparison of present-day spatial extent of main lithologies in the catchment of the different drainage systems versus proportion of DZ ages corresponding to source rocks. Note that, although as a fraction of the catchment the Blackwood/Scott drainage does not cover as much of the Perth Basin as the Donnelly River, it exceeds it four times in terms of area.; PB –Perth Basin, PJO – Pinjarra Orogen; AFO – Albany-Fraser Orogen; YC – Yilgarn Craton. (B) Zirconium (Zr) content of the different source. Data have been obtained from the online database of the Geological Survey of Western Australia (*dmp.wa.gov.au/Geochem*), only igneous and metamorphic rocks >60 wt% SiO_2 have been used; LC – Leeuwin Complex, SWT – South West Terrane, CI – Confidence interval, n – number of analyses.

that sedimentary recycling of the Cenozoic sediment veneer appears to be more important than recycling of underlying Mesozoic and Palaeozoic strata of the Perth Basin (Fig. 3). However, given the proven zircon cargo within the Perth Basin, these sedimentary rocks may have been a source of DZ for pre-Pleistocene sediments of the SCP, which are in turn inferred to be the dominant source of modern fluvial DZ. Sedimentary recycling thus masks propagation of geological signals from source-to-sink, i.e., providing very limited information about the crystalline basement catchment geology. This is contrary to the often-assumed representativeness of fluvial sands for their catchment (Caracciolo, 2020), suggesting that fluvial samples need to be carefully evaluated based on their geological setting to avoid misinterpretation.

5.3. Environmental controls of coastal plain detrital zircon composition

Coastal morphology and swell direction affect the dispersion of DZ in littoral sediments of the study area. The negative correlation of PJO- and AFO-derived DZ is suggestive of a net west-to-east sediment longshore drift system, consistent with the dominant swell direction (Fig. 5A) and corresponding increasing roundness of detrital grains (Fig. S1). The negative correlation is also consistent with decreasing similarity of littoral DZ age spectra towards the east when compared to the most western DZ age spectra (Fig. 5B). The steady increase of AFO- (and decline of PJO-) derived DZ is best explained with progressive dilution of the PJO longshore drift

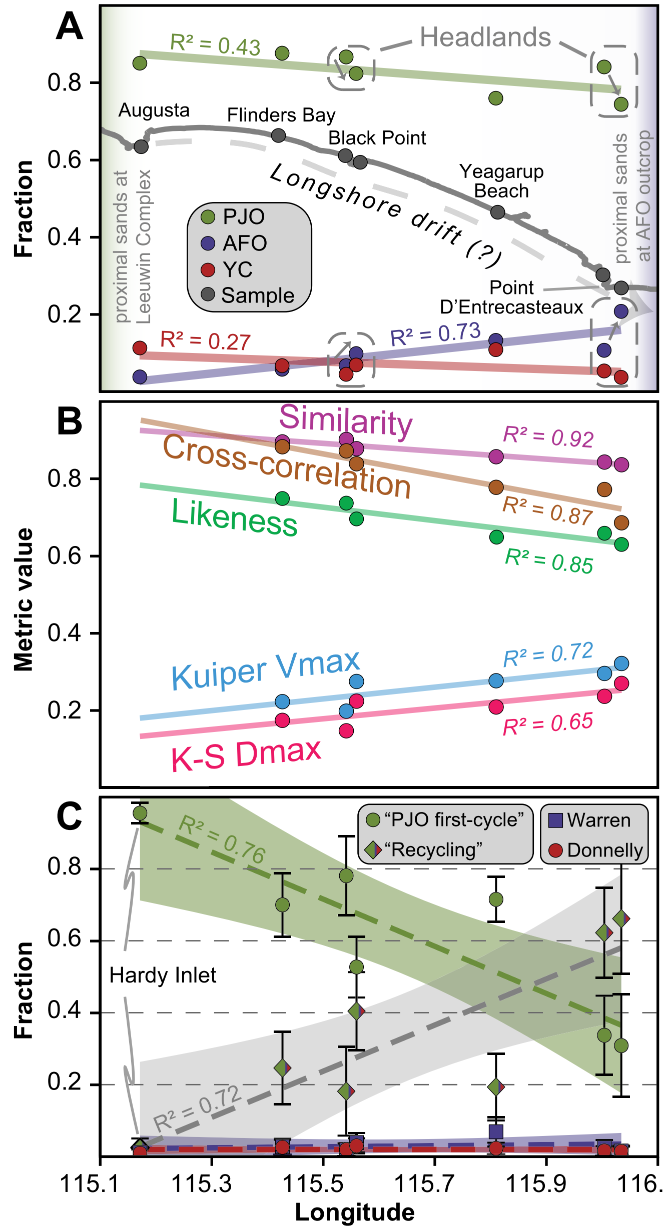

Fig. 5. (A) Spatial variation of littoral DZ sample age modes assigned to source rocks; PJO – Pinjarra Orogen; AFO – Albany-Fraser Orogen; YC – Yilgarn Craton. (B) Different metrics used in DZ geochronology to compare similarity between samples. All values refer to the comparison with the most western beach sample near Augusta. (C) Results of inverse Monte Carlo modelling (Sundell and Saylor, 2017) using K–S statistics to constrain contribution of different idealised sources. The "PJO first-cycle" fraction is likely to be overestimated by the model as the "PJO first-cycle" parameter is not entirely first-cycle sand, but contains grains not representing PJO first-cycle sand (e.g., AFO-derived grains). Note: most western sample is Hardy Inlet (different to Fig. 5A).

signal and increasing proximity of AFO bedrock at the eastern end of the study area. The DZ composition along the coast is also influenced by the presence of headlands. At both Black Point and Point D'Entrecasteaux headlands, the relative abundance of PJO-derived DZ declines from west to east, whereas the relative AFO-derived DZ abundance increases (Fig. 5A). Therefore, headlands appear to generate a shift of DZ age distributions and influence propagation of DZ populations along the shore. This is consistent with clustering in multidimensional scaling (MDS) space, which corresponds to the eastern (Yeagarup Beach) and western part (Flinders Bay) of the study area that are separated by the Black Point Headland (Fig. 1C; Fig. 3B).

The coastally exposed PJO is subject to one of the highest wave energies in Australia (Porter-Smith et al., 2004). Thus, preferential erosion of coastal outcrops supplying first-cycle sands and transportation by the eastward sediment longshore drift system, as well as increased zircon fertility (Fig. 4B), are interpreted to contribute to the widespread PJO-derived DZ in littoral sediments across the SCP. However, as the modern littoral sands exhibit significant occurrences of non-PJO aged grains, supply of multi-cycle DZ, either by riverine discharge or sedimentary recycling of older coastal sediments, are expected to influence DZ composition along with enhancing single source dominance. To test the contribution of direct sourcing versus sedimentary recycling in modern-day littoral sands, we assume that the DZ from Augusta, proximal to the outcropping PJO (Fig. 1C), are the best approximation of first-cycle sands derived from the PJO. Moreover, we assume the Blackwood and Scott river samples DZ approximate the DZ age distribution of the Cenozoic sediment veneer (section 5.2). Following these assumptions, we model the contribution from "PJO first-cycle" (source rock proximal sand derived by coastal erosion), "recycling" (Blackwood and Scott river sand), and "catchment erosion" represented by the Donnelly, and Warren rivers (Fig. 5C). To constrain mixing proportions, we apply an inverse Monte-Carlo model using the MATLAB code written by Sundell and Saylor (2017). As expected by sediment supply (Fig. 1B), the model attributes limited contributions to the littoral DZ age distribution by the Donnelly River (YC signal) and Warren River (AFO signal). An exception is the Yeagarup Beach DZ (sample YGP001) showing a small but distinct spike in Warren River contribution, which is interpreted to relate to local influence by the sample's proximity (*c.* 2 km) to the Warren River mouth. The proxies for PJO-derived first-cycle sand and recycled sand show linear decreases and increases, respectively. Such patterns imply first-cycle sediment is particularly dominant proximal to the outcropping PJO and becomes less evident with greater distance.

Ultimately, DZ ages and model results suggest DZ composition becomes substantially more influenced by erosion of coastal sediments eastwards and, that the minor drainage systems (Donnelly and Warren) do not influence the littoral DZ cargo considerably. Furthermore, this implies that autogenic processes (i.e., onshore transportation, sediment storage, and sedimentary recycling) are a first-order control on DZ composition in this setting. Integrated with preferential erosion of one source, and minimal sediment supply of other sources, coastal plains' DZ age distributions may not be representative for the extent of bedrock of their catchment, but are essentially the consequence of environmental controls, i.e., significantly biased. However, if this bias, fundamentally dictated by sedimentary processes, is recognized, it can be used to assess intermediate sediment storage and sediment pathways (Caracciolo, 2020).

5.4. Source-normalized α-dose: a new tool to quantify transport and recycling in DZ geochronology

Source-normalized α-dose compares α-dose (that is a first-order approximation of the degree of metamictization) of individual DZ grains to the average α-dose of grains within its source rock. The concept primarily assumes selective removal of less durable (i.e., metamict) zircon grains during sedimentary processes as demonstrated by previous studies (Malusà et al., 2013; Markwitz and Kirkland, 2018; Resentini et al., 2020; Sircombe and Stern, 2002). The difference in the α-dose of zircon grains that develops between ultimate source and sink is a measure of the active time in the sedimentary system, i.e., the total exposure to processes responsible for the removal of metamict grains. Thus, DZ populations that were subject to multiple sedimentary recycling events are expected to exhibit significantly lower α-dose values compared to grains in pristine source rocks that have not experienced destructive dissolution and abrasion processes of a sedimentary cycle. Accordingly, recycled zircon populations, or those with protracted sedimentary histories are expected to exhibit source-normalized α-dose values <1. Conversely, first-cycle sands, which do not experience considerable transport and reworking, are hypothesised to show values of *c.* 1. Consequently, source-normalized α-dose may help to constrain the degree of transport and reworking of DZ age modes corresponding to distinct sources. Age bins of DZ and source rock zircons used for calculation of source-normalized α-dose are given in Supplementary Material S1.

The high similarity of the α-dose values of the PJO age mode in the Augusta beach DZ population and its source rock (expressed by a source-normalized α-dose of *c.* 1; Fig. 6A) suggests that this population has not been significantly modified, and is likely first-cycle. The significant decline of source-normalized α-dose values of PJO-derived DZ (source based on U–Pb ages) from the most western to all eastern littoral samples (Fig. 6B) is consistent with (i) mechanical breakdown during longshore transportation and (ii) increasing contribution of multi-cycle DZ derived from older coastal strata. Significant supply of multi-cycle DZ (both through the Blackwood-Scott system and contiguous coast-backing sediment reservoirs) from the coastal plain is consistent with the significant decline in source-normalized α-dose east of Augusta. These sediments have spent considerable time within the coastal system during Cenozoic sea-level fluctuations and have consequently been subject to protracted physical transport attrition, chemical weathering during storage, and multiple sedimentation and erosion events capable of destroying metamict zircon grains. Higher source-normalized α-dose values are evident for rivers that more accurately match their catchment geology (Donnelly and Warren) consistent with higher proportions of minimally transported material and the general applicability of source-normalized α-dose to distinguish proportions of first- and multi-cycle DZ. High α-dose of the YC basement (Fig. 6C) in combination with lower fertility can in parts explain scarcity of YC-derived grains (although YC by far exceeds PJO and AFO in terms of present-day area) in the littoral sediments (Fig. 2) and in other clastic strata of the Perth Basin (Olierook et al., 2019). However, comparatively low abundance of Archean DZ is also the result of generally increasing zircon fertility per mass of magma through time (Keller et al., 2017).

The multi-cycle nature of AFO-derived DZ is suggested by the absence of AFO source rocks in the river catchments, and consistent with low source-normalized α-dose in the Blackwood/Scott River (*c.* 0.4). This is supported by comparison to PJO-derived DZ in the same samples that show higher values and are, based on source proximity, less likely to be affected by sedimentary recycling than the AFO-derived DZ. AFO-derived DZ in the Perth Basin are believed to be in part sourced by recycling of a now-fully eroded (or not sampled) sediment veneer covering the YC (e.g., Olierook et al., 2019; Veevers et al., 2005). Low source-normalized α-dose value of AFO-derived DZ in the southern Perth Basin support a multi-cycle origin (Fig. 7A). The southern Perth Basin source-normalized α-dose is higher compared to the present-day Blackwood/Scott River (although low-*n* limits interpretative power). Therefore, this observation further supports the interpretation that the lower source-normalized α-dose AFO-derived DZ population of the present-day Blackwood/Scott River has been subject to selective removal of higher α-dose zircon grains within the underlying Perth Basin and coastal plain facies during recycling. Consequently, comparison of DZ and source α-dose (documented through source-normalized α-dose) aids in discrimination of first-versus multi-cycle contribution in DZ populations, using chemistry typically captured during routine U–Pb geochronology. Fur-

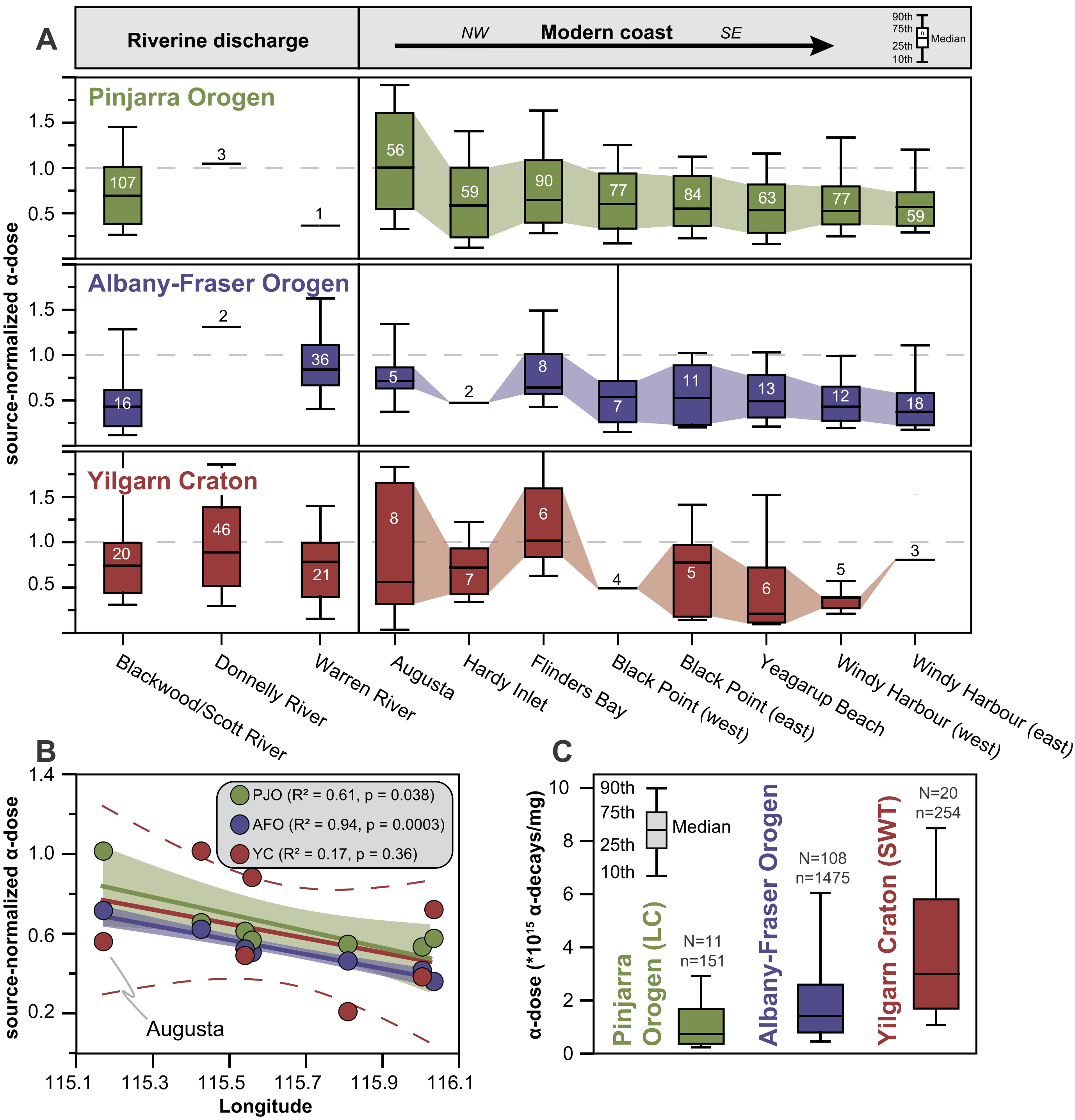

Fig. 6. (A) Boxplots of source-normalized α-dose of modern sediments for assigned source rocks, for instance, Pinjarra Orogen box plots (green) include only DZ that display ages corresponding to the Pinjarra Orogen. No boxplot (but median) is shown if n (number of concordant analyses) is <5. (B) Median of source-normalized α-dose for littoral samples and linear regressions; PJO – Pinjarra Orogen; AFO – Albany-Fraser Orogen; YC – Yilgarn Craton. (C) α-dose values of zircon grains from interpreted source rocks; LC – Leeuwin Complex; SWT – South West Terrane; N – number of samples; n – number of analyses. Source-normalized α-dose values of DZ are given in Supplementary Table S4 in Supplementary Material S2.

thermore, comparison with possible intermediate sediment storage reservoirs indicates that source-normalized α-dose can be applied in the deep-time geological record.

5.5. Implications for sedimentary provenance analysis in the deep-time geological record

To validate the use of source-normalized α-dose in DZ provenance analysis more broadly, we test this tool on DZ populations derived from the Grenville Orogen, North America. The dominance of Grenville detritus in Phanerozoic clastic strata in North America, specifically in former Laurentia, is well-studied and assumed to be primarily the result of exceptional zircon fertility and multiple sedimentary recycling episodes (e.g., Moecher and Samson, 2006; Potter-McIntyre et al., 2018; Zotto et al., 2020). Moecher et al. (2019) proved recycling using textures of detrital diagenetic monazite. Widespread sedimentary recycling processes are also supported through indirect observations, i.e., by comparison with

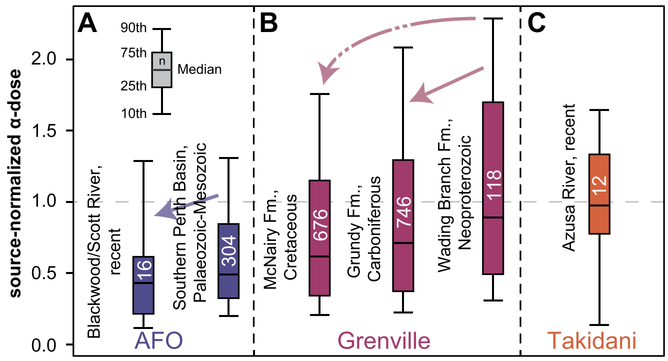

Fig. 7. Boxplots of source-normalized α-dose to track progressive sedimentary recycling of (A) Albany-Fraser Orogen (AFO) derived DZ in modern fluvial sands (this study) and Mesozoic basement in SW Australia (data from Olierook et al. (2019) and references therein), (B) Grenville-derived DZ in different clastic sedimentary rocks from former Laurentia: McNairy Fm. (Potter-McIntyre et al., 2018), Grundy Fm. (Zotto et al., 2020), Wading Branch Fm. (Chakraborty et al., 2012); source rock data ($n = 398$) from Southworth et al. (2010); age bin = 1190–1020 Ma, and (C) Takidani-intrusion-derived first-cycle river sands (source rock ($n = 17$) and DZ data from Ito et al. (2017); age bin = 1.75–1.23 Ma); n – number of analyses.

older strata exposing similar DZ age spectra (e.g., Potter-McIntyre et al., 2018). Therefore, well-established sedimentary recycling relationships allow for testing source-normalized α-dose as a general application in DZ geochronology.

Results suggest source-normalized α-dose establishes the same relationships as other measures of cyclicity, when applied to ancient geological settings. The basal Lower Ocoee Supergroup (Wading Branch Formation) is interpreted to be sourced primarily from the underlying Mesoproterozoic Grenville basement (Chakraborty et al., 2012). Its Grenville-derived DZ population source-normalized α-dose of *c.* 0.9 supports limited transport and a predominant first-cycle origin (Fig. 7B). Zotto et al. (2020) advocated that the Neoproterozoic Lower Ocoee Supergroup and Cambrian lithologies are the main source of DZ supplying the proximal Carboniferous Grundy Formation, which shows a significantly lower source-normalized α-dose of its Grenville-derived DZ population (*c.* 0.7). Hence, source-normalized α-dose captures a multi-cycle history that agrees with the previously published interpretation. Moreover, the source-normalized α-dose of younger fluvial strata of the Mississippi embayment (Cretaceous McNairy Formation) shows even lower values (*c.* 0.6; Fig. 7B). The continuous decline of source-normalized α-dose is interpreted to document progressive sedimentary recycling and transportation. Furthermore, the 10th percentile α-dose is relatively constant, even though the 90th percentile drops significantly in the Grenville-derived DZ, which suggests that the metric relates to a geologically meaningful process: the destruction of more labile metamict grains.

To test results of source-normalized α-dose in the absence of sedimentary recycling, we compared the α-dose of Takidani granodiorite zircon crystals and DZ of the same age within the Azusa River in Japan using data published by Ito et al. (2017). The river sample was taken in close proximity to its igneous source; therefore, it reflects a first-cycle sand directly sourced from the intrusion. As expected, based on apparent relationships, the first-cycle sands of the modern Azusa River in Japan display a source-normalized α-dose of *c.* 1, i.e., capturing the same variability of zircon α-dose as the proximal source rock (Fig. 7C).

In addition to evaluation of the multi-cycle proportion of individual DZ age modes, differences in source-normalized α-dose between two DZ modes may allow quantification of information loss, e.g., which age mode was more affected by sedimentary recycling (i.e., loss of metamict grains) and, therefore, will be less preserved in the detrital record. In this study, our findings suggest no preferential information loss between the main PJO and AFO DZ populations (Sircombe and Stern, 2002; Fig. 6B). However, being an internal mechanism that fundamentally explores loss of more labile grains through time, source-normalized α-dose allows for replication of results derived by other mineral proxies, i.e., it provides first order constraints on sedimentary transport and recycling of DZ.

5.6. Application and limitations

A fundamental assumption of source-normalized α-dose application is the accurate discrimination of the source using the DZ age fingerprint or other proxies (e.g., integrated geochemical techniques). That is, only age populations that can be traced back to a specific source allow for source-normalized α-dose calculation. Therefore, the use of this metric is favoured for diversified age spectra of distinct sources. Likewise, regions of well-characterised basement rocks (i.e., sufficient numbers of analyses) that capture their source natural variability, will provide more accurate results. Non-normalized α-dose values cannot be compared between different age modes, i.e., preferential removal of DZ populations, as a proxy for bias, cannot be detected. However, in the absence of suitable source rock data, a simple comparison of α-dose values of the same distinct age mode between samples may be capable of demonstrating relative recycling. As with source-normalized values, a decline of high α-dose grains through successively younger depositional units should be considered an indication of likely sedimentary recycling.

The concept does not factor in annealing as part of the grain history (Nasdala et al., 2001), and consequently considers continuous accumulation of α-decay damage from crystallization. Therefore, source-normalized α-dose is expected to represent a minimum constraint on the degree of multi-cyclicity. However, in this study the observed disparities in source-normalized α-dose between DZ populations are clearly best explained by removal of highly metamict grains, suggesting annealing is secondary to the sedimentary recycling signal.

6. Conclusions

An investigation of modern coastal plain sediments reveals environmental control and progressive sedimentary recycling dictating DZ composition. The relative proportions of DZ age modes in the major drainage system flowing through the Scott Coastal Plain do not match the areal extent of source rocks in the catchment(s), but are similar to the DZ age mode proportions within Cenozoic strata, thus challenging the use of fluvial DZ age spectra as a measure of catchment geology. Supply of first-cycle sands from a basement outcrop, which is exposed to preferential erosion, *via* a net west-to-east longshore drift system, has been identified controlling DZ on a local scale. However, the dominant mechanism controlling overall coastal plain DZ composition is interpreted to be progressive recycling of sediments in successive coastal systems. Ultimately, these findings demonstrate intrinsic controls of DZ composition in coastal plains, resulting in prevalence of multi-cycle DZ. This process buffers propagation of primary geological signals from source-to-sink limiting the use of the detrital record as a direct fingerprint of the source area. Consequently, these results highlight the need for careful evaluation of first- and multi-cycle DZ signals to maintain a meaningful geological interpretation.

Source-normalized α-dose, a novel metric comparing α-dose of DZ and zircon crystals retained in their crystalline source rocks, constrains the degree of grain transport and recycling. Selective removal of more labile (i.e., metamict) zircon grains, correlating with active time in the sedimentary system, leads to a decrease of source-normalized α-dose values (Fig. 8). A value close to 1 is characteristic of first-cycle material and reduced transportation

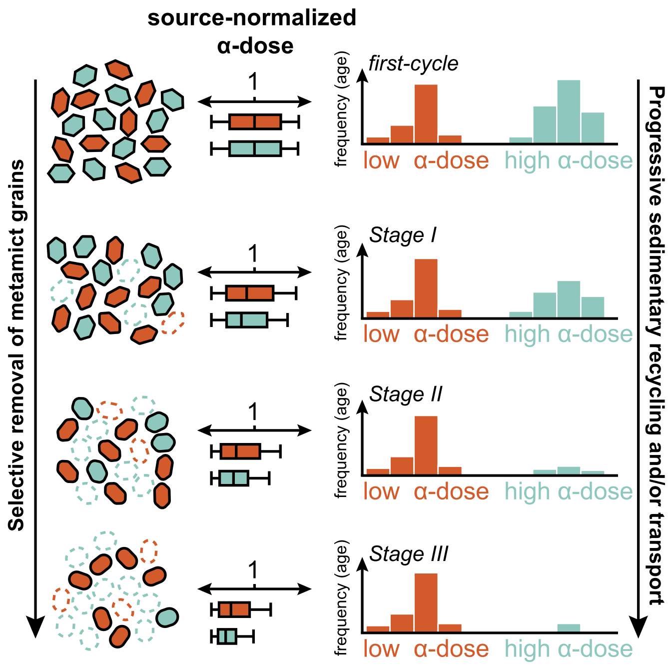

Fig. 8. Schematic visualization of the concept of source-normalized α-dose. Progressive sedimentary recycling and/or transport of DZ will lead to increased selective removal of metamict grains, which results in lower source-normalized α-dose values. Stages I–III track shift of abundance of low and high α-dose DZ through multiple episodes of sedimentary recycling.

of grains, with values progressively decreasing in tandem with progressive transportation and reworking. Understanding complex grain histories can improve the interpretive power of provenance analysis using DZ in multi-cycle sedimentary systems by filtering for primary geological processes in the source area. Source-normalized α-dose can be readily applied to published DZ datasets and will improve recognition of a significant bias in DZ geochronology due to the multi-cycle nature of zircon.

CRediT authorship contribution statement

Maximilian Dröllner: Conceptualization, Formal analysis, Investigation, Methodology, Visualization, Writing – original draft. **Milo Barham:** Conceptualization, Funding acquisition, Supervision, Writing – review & editing. **Christopher L. Kirkland:** Conceptualization, Funding acquisition, Supervision, Writing – review & editing.

Declaration of competing interest

The authors declare that they have no known competing financial interests or personal relationships that could have appeared to influence the work reported in this paper.

Acknowledgements

This research was supported by MRIWA grant M551 in collaboration with Iluka Resources. We would like to thank Maike Schulz and Andreas Zametzer for assisting with fieldwork, Noreen Evans and Brad McDonald for help with LA-ICP-MS analysis, and David Sleigh and Rohan Hine for insightful discussions. We also thank the Department of Biodiversity, Conservation and Attractions (Donnelly District) and Mark Virgo for sampling permission and advice regarding access to sampling sites. Furthermore, we thank an anonymous landowner for access near Flinders Bay. Journal reviews by Alberto Resentini and an anonymous reviewer, as well as editorial handling by Alex Webb, are greatly appreciated. Part of this research was undertaken using the electron microscope instrumentation (ARC LE190100176 & LE140100150) at the John de Laeter Centre, Curtin University. Research in the GeoHistory Facility (John de Laeter Centre) is enabled by AuScope (auscope.org.au) and the Australian Government via the National Collaborative Research Infrastructure Strategy (NCRIS).

Appendix A. Supplementary material

Supplementary material related to this article can be found online at https://doi.org/10.1016/j.epsl.2021.117346.

References

Baddock, L.J., 1995. Geology and Hydrogeology of the Scott Coastal Plain, Perth Basin. Geological Survey of Western Australia, Perth.
Balan, E., Neuville, D.R., Trocellier, P., Fritsch, E., Muller, J.-P., Calas, G., 2001. Metamictization and chemical durability of detrital zircon. Am. Mineral. 86 (9), 1025–1033.
Barham, M., Kirkland, C.L., Hovikoski, J., Alsen, P., Hollis, J., Tyrrell, S., 2021. Reduce or recycle? Revealing source to sink links through integrated zircon–feldspar provenance fingerprinting. Sedimentology 68 (2), 531–556.
Baxter, J.L., 1977. Heavy Mineral Sand Deposits of Western Australia. Mineral Resources Bulletin, vol. 10. Geological Survey of Western Australia, Perth.
Blatt, H., 1967. Provenance determinations and recycling of sediments. J. Sediment. Res. 37.
Blöthe, J.H., Korup, O., 2013. Millennial lag times in the Himalayan sediment routing system. Earth Planet. Sci. Lett. 382, 38–46.
Caracciolo, L., 2020. Sediment generation and sediment routing systems from a quantitative provenance analysis perspective: review, application and future development. Earth-Sci. Rev. 209, 103226.
Cawood, P.A., Hawkesworth, C.J., Dhuime, B., 2012. Detrital zircon record and tectonic setting. Geology 40 (10), 875–878.
Chakoumakos, B.C., Murakami, T., Lumpkin, G.R., Ewing, R.C., 1987. Alpha-decay–induced fracturing in zircon: the transition from the crystalline to the metamict state. Science 236 (4808), 1556–1559.
Chakraborty, S., Moecher, D.P., Samson, S.D., 2012. Provenance of the Lower Ocoee Supergroup, eastern Great Smoky Mountains. Geol. Soc. Am. Bull. 124 (7–8), 1278–1292.
Chew, D., O'Sullivan, G., Caracciolo, L., Mark, C., Tyrrell, S., 2020. Sourcing the sand: accessory mineral fertility, analytical and other biases in detrital U–Pb provenance analysis. Earth-Sci. Rev. 202, 103093.
Collins, A.S., 2003. Structure and age of the northern Leeuwin Complex, Western Australia: constraints from field mapping and U–Pb isotopic analysis. Aust. J. Earth Sci. 50 (4), 585–599.
Covault, J.A., Romans, B.W., Fildani, A., McGann, M., Graham, S.A., 2010. Rapid climatic signal propagation from source to sink in a Southern California Sediment-routing system. J. Geol. 118 (3), 247–259.
Dickinson, W.R., Gehrels, G.E., 2008. U–Pb ages of detrital zircons in relation to paleogeography: Triassic paleodrainage networks and sediment dispersal across Southwest Laurentia. J. Sediment. Res. 78 (12), 745–764.
Dröllner, M., Barham, M., Kirkland, C.L., Ware, B., 2021. Every zircon deserves a date: selection bias in detrital geochronology. Geol. Mag. 158 (6), 1135–1142.
Dumitru, T.A., 2016. A new zircon concentrating table designed for geochronologists. In: AGU Fall Meeting Abstracts.
Eliot, I., Nutt, C., Gozzard, B., Higgins, M., Buckley, E., Bowyer, J., 2011. Coastal compartments of Western Australia: a physical framework for marine and coastal planning. In: Report to the Departments of Environment & Conservation, Planning and Transport. Damara WA Pty Ltd, Geological Survey of Western Australia and Department of Environment & Conservation. Western Australia.
Fülöp, R.-H., Codilean, A.T., Wilcken, K.M., Cohen, T.J., Fink, D., Smith, A.M., Yang, B., Levchenko, V.A., Wacker, L., Marx, S.K., Stromsoe, N., Fujioka, T., Dunai, T.J., 2020. Million-year lag times in a post-orogenic sediment conveyor. Sci. Adv. 6 (25), eaaz8845.
Holland, H.D., Gottfried, D., 1955. The effect of nuclear radiation on the structure of zircon. Acta Crystallogr. 8 (6), 291–300.
Huber, B., Bahlburg, H., Berndt, J., Dunkl, I., Gerdes, A., 2018. Provenance of the surveyor fan and precursor sediments in the Gulf of Alaska—implications of a combined U–Pb, (U–Th)/He, Hf, and rare Earth element study of detrital zircons. J. Geol. 126 (6), 577–600.
Ito, H., Spencer, C.J., Danišík, M., Hoiland, C.W., 2017. Magmatic tempo of Earth's youngest exposed plutons as revealed by detrital zircon U–Pb geochronology. Sci. Rep. 7 (1), 12457.
Keller, C.B., Boehnke, P., Schoene, B., 2017. Temporal variation in relative zircon abundance throughout Earth history. Geochem. Perspect. Lett., 179–189.
Kirkland, C.L., Spaggiari, C.V., Pawley, M.J., Wingate, M., Smithies, R.H., Howard, H.M., Tyler, I.M., Belousova, E.A., Poujol, M., 2011. On the edge: U–Pb, Lu–Hf, and Sm–Nd data suggests reworking of the Yilgarn craton margin during formation of the Albany-Fraser Orogen. Precambrian Res. 187 (3–4), 223–247.

Lewis, C.J., 2017. SHRIMP U–Pb detrital zircon ages from GSWA Harvey 1, In: Western Australia: July 2013 - June 2015. Record 2017/20. Geoscience Australia, Canberra.

Malusà, M.G., Carter, A., Limoncelli, M., Villa, I.M., Garzanti, E., 2013. Bias in detrital zircon geochronology and thermochronometry. Chem. Geol. 359, 90–107.

Markwitz, V., Kirkland, C.L., 2018. Source to sink zircon grain shape: constraints on selective preservation and significance for Western Australian Proterozoic basin provenance. Geosci. Front. 9 (2), 415–430.

Meinhold, G., Morton, A.C., Fanning, C.M., Frei, D., Howard, J.P., Phillips, R.J., Strogen, D., Whitham, A.G., 2011. Evidence from detrital zircons for recycling of Mesoproterozoic and Neoproterozoic crust recorded in Paleozoic and Mesozoic sandstones of southern Libya. Earth Planet. Sci. Lett. 312 (1–2), 164–175.

Moecher, D.P., Samson, S.D., 2006. Differential zircon fertility of source terranes and natural bias in the detrital zircon record: implications for sedimentary provenance analysis. Earth Planet. Sci. Lett. 247 (3–4), 252–266.

Moecher, D.P., Kelly, E.A., Hietpas, J., Samson, S.D., 2019. Proof of recycling in clastic sedimentary systems from textural analysis and geochronology of detrital monazite: implications for detrital mineral provenance analysis. Bulletin 131 (7–8), 1115–1132.

Mole, D.R., Kirkland, C.L., Fiorentini, M.L., Barnes, S.J., Cassidy, K.F., Isaac, C., Belousova, E.A., Hartnady, M., Thebaud, N., 2019. Time-space evolution of an Archean craton: a Hf-isotope window into continent formation. Earth-Sci. Rev. 196, 102831.

Murakami, T., Chakoumakos, B.C., Ewing, R.C., Lumpkin, G.R., Weber, W.J., 1991. Alpha-decay event damage in zircon. Am. Mineral. 76 (9–10), 1510–1532.

Nasdala, L., Wenzel, M., Vavra, G., Irmer, G., Wenzel, T., Kober, B., 2001. Metamictisation of natural zircon: accumulation versus thermal annealing of radioactivity-induced damage. Contrib. Mineral. Petrol. 141 (2), 125–144.

Nyberg, B., Gawthorpe, R.L., Helland-Hansen, W., 2018. The distribution of rivers to terrestrial sinks: implications for sediment routing systems. Geomorphology 316, 1–23.

Olierook, H.K., Barham, M., Fitzsimons, I.C., Timms, N.E., Jiang, Q., Evans, N.J., McDonald, B.J., 2019. Tectonic controls on sediment provenance evolution in rift basins: detrital zircon U–Pb and Hf isotope analysis from the Perth Basin, Western Australia. Gondwana Res. 66, 126–142.

Phillips, J.D., Slattery, M.C., 2006. Sediment storage, sea level, and sediment delivery to the ocean by coastal plain rivers. Prog. Phys. Geogr.: Earth Environ. 30 (4), 513–530.

Porter-Smith, R., Harris, P.T., Andersen, O.B., Coleman, R., Greenslade, D., Jenkins, C.J., 2004. Classification of the Australian continental shelf based on predicted sediment threshold exceedance from tidal currents and swell waves. Mar. Geol. 211 (1–2), 1–20.

Potter-McIntyre, S.L., Breeden, J.R., Malone, D.H., 2018. A Maastrichtian birth of the Ancestral Mississippi River system: evidence from the U–Pb detrital zircon geochronology of the McNairy Sandstone, Illinois, USA. Cretac. Res. 91, 71–79.

Rahl, J.M., Reiners, P.W., Campbell, I.H., Nicolescu, S., Allen, C.M., 2003. Combined single-grain (U–Th)/He and U/Pb dating of detrital zircons from the Navajo Sandstone, Utah. Geology 31 (9), 761–764.

Resentini, A., Andò, S., Garzanti, E., Malusà, M.G., Pastore, G., Vermeesch, P., Chanvry, E., Dall'Asta, M., 2020. Zircon as a provenance tracer: coupling Raman spectroscopy and U Pb geochronology in source-to-sink studies. Chem. Geol. 555, 119828.

Romans, B.W., Castelltort, S., Covault, J.A., Fildani, A., Walsh, J.P., 2016. Environmental signal propagation in sedimentary systems across timescales. Earth-Sci. Rev. 153, 7–29.

Short, A.D., 2010. Sediment transport around Australia—sources, mechanisms, rates, and barrier forms. J. Coast. Res. 26 (3), 395–402.

Sircombe, K.N., Freeman, M.J., 1999. Provenance of detrital zircons on the Western Australia coastline—implications for the geologic history of the Perth basin and denudation of the Yilgarn craton. Geology 27 (10), 879–882.

Sircombe, K.N., Stern, R.A., 2002. An investigation of artificial biasing in detrital zircon U–Pb geochronology due to magnetic separation in sample preparation. Geochim. Cosmochim. Acta 66 (13), 2379–2397.

Southworth, S., Aleinikoff, J.N., Tollo, R.P., Bailey, C.M., Burton, W.C., Hackley, P.C., Fanning, C.M., 2010. Mesoproterozoic magmatism and deformation in the northern Blue Ridge, Virginia and Maryland: application of SHRIMP U–Pb geochronology and integrated field studies in the definition of Grenvillian tectonic history. In: Tollo, R.P., Bartholomew, M.J., Hibbard, J.P., Karabinos, P.M. (Eds.), From Rodinia to Pangea: The Lithotectonic Record of the Appalachian Region. Geological Society of America.

Spencer, C.J., Kirkland, C.L., Roberts, N.M.W., 2018. Implications of erosion and bedrock composition on zircon fertility: examples from South America and Western Australia. Terra Nova 30 (4), 289–295.

Steiger, R.H., Jäger, E., 1977. Subcommission on geochronology: convention on the use of decay constants in geo- and cosmochronology. Earth Planet. Sci. Lett. 36 (3), 359–362.

Sundell, K.E., Saylor, J.E., 2017. Unmixing detrital geochronology age distributions. Geochem. Geophys. Geosyst. 18 (8), 2872–2886.

Syvitski, J.P.M., Milliman, J.D., 2007. Geology, geography, and humans battle for dominance over the delivery of fluvial sediment to the coastal ocean. J. Geol. 115 (1), 1–19.

Tyrrell, S., Leleu, S., Souders, A.K., Haughton, P.D., Daly, J.S., 2009. K-feldspar sand-grain provenance in the Triassic, West of Shetland: distinguishing first-cycle and recycled sediment sources? Geol. J. 44 (6), 692–710.

Veevers, J.J., Saeed, A., Belousova, E.A., Griffin, W.L., 2005. U–Pb ages and source composition by Hf-isotope and trace-element analysis of detrital zircons in Permian sandstone and modern sand from southwestern Australia and a review of the paleogeographical and denudational history of the Yilgarn Craton. Earth-Sci. Rev. 68 (3–4), 245–279.

Zotto, S.C., Moecher, D.P., Niemi, N.A., Thigpen, J.R., Samson, S.D., 2020. Persistence of Grenvillian dominance in Laurentian detrital zircon age systematics explained by sedimentary recycling: evidence from detrital zircon double dating and detrital monazite textures and geochronology. Geology 48 (8), 792–797.